LA-UR-13-21747
Approved for public release; distribution is unlimited.

Title: The Contour Method

Author(s): Prime, Michael B.
DeWald, Adrian T.

Intended for: Practical Residual Stress Measurement Methods, G. S. Schajer, (ed.), Wiley-Blackwell

M. B. Prime and A.T. DeWald, 2013, "The Contour Method," Chapter 5 in Practical Residual Stress Measurement Methods, G. S. Schajer, (ed.), Wiley-Blackwell, pp. 109-138.

Disclaimer:
Los Alamos National Laboratory, an affirmative action/equal opportunity employer,is operated by the Los Alamos National Security, LLC for the National NuclearSecurity Administration of the U.S. Department of Energy under contract DE-AC52-06NA25396. By approving this article, the publisher recognizes that the U.S. Government retains nonexclusive, royalty-free license to publish or reproduce the published form of this contribution, or to allow others to do so, for U.S. Government purposes. Los Alamos National Laboratory requests that the publisher identify this article as work performed under the auspices of the U.S. Departmentof Energy. Los Alamos National Laboratory strongly supports academic freedom and a researcher's right to publish; as an institution, however, the Laboratory does not endorse the viewpoint of a publication or guarantee its technical correctness.

M. B. Prime and A.T. DeWald, "The Contour Method,"
Chapter 5 in *Practical Residual Stress Measurement Methods*,
G. S. Schajer, (ed.), Wiley-Blackwell, 2013, pp. 109-138.

5. THE CONTOUR METHOD

Michael B. Prime, Los Alamos National Laboratory, Los Alamos, NM 87545, USA
Adrian T. DeWald, Hill Engineering, LLC, Rancho Cordova, CA 95670, USA

5.1 Introduction

5.1.1 *Contour method overview*

The contour method, which is based upon solid mechanics, determines residual stress through an experiment that involves carefully cutting a specimen into two pieces and measuring the resulting deformation due to residual stress redistribution. The measured displacement data are used to compute residual stresses through an analysis that involves a finite element model of the specimen. As part of the analysis, the measured deformation is imposed as a set of displacement boundary conditions on the model. The finite element model accounts for the stiffness of the material and part geometry to provide a unique result. The output is a two-dimensional map of residual stress normal to the measurement plane. The contour method is particularly useful for complex, spatially varying residual stress fields that are difficult (or slow) to map using conventional point wise measurement techniques. For example, the complex spatial variations of residual stress typical of welds are well-characterized using the contour method.

Contour method measurements are typically performed on metallic parts, which can be cut using a wire electric discharge machine (EDM). There are no specific size restrictions, but the measurement signal (displacement) scales with specimen size and performing measurements on parts smaller than 5 mm by 5 mm in cross-section requires extreme precision. There are no restrictions on the shape of the specimen due to the fact that complex geometry is accounted for using a finite element model of the part.

The contour method is the youngest method covered in this book, having been first presented at a conference in 2000 [1] and then in a journal in 2001 [2]. Therefore, consensus best practices are not as well established as for other methods. A basic measurement procedure is provided along with comments about potential alternate approaches, with references for further reading.

5.1.2 *Bueckner's principle*

The contour method theory is a variation on Bueckner's superposition principle. Bueckner presented the relevant theory in 1958 [3] and discussed it further in later publications [4,5]. However, Buckner's papers present no figure like those presented in this chapter. The apparent first use of such a figure for Bueckner's principle was by Barenblatt in 1962 [6]. A very similar principle and figure was presented independently in Paris' landmark 1961 paper on fatigue crack growth [7], and he credits the principle to a 1957 report he wrote for The Boeing Company. It is conceivable that other work predates that of Bueckner and Paris. Bueckner's principle is also quite similar to the better known inclusion problem presented by Eshelby in

1957 [8]. In any case, Bueckner's principle is indispensable in fracture mechanics work [9] and has proven invaluable when used appropriately.

5.2 Measurement Principle

5.2.1 *Ideal theoretical implementation*

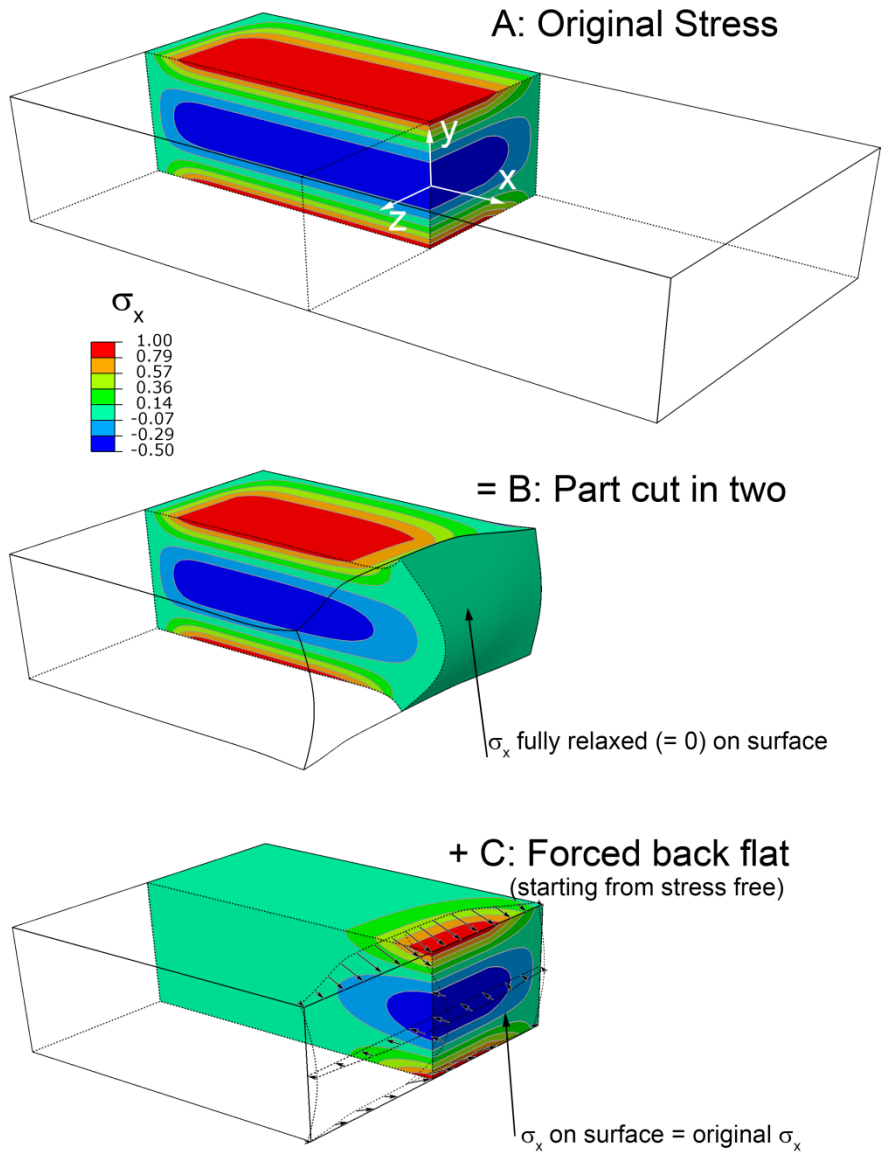

Figure 5.1. Superposition principle for the contour method. Stresses are plotted on one quarter of the original body.

The ideal theoretical implementation of the contour method is presented here first before discussing the assumptions and approximations that will be required for a practical implementation. Figure 5.1 presents a 3-D illustration for a thick plate in which the longitudinal stress varies parabolically through the thickness of a plate. Fig.1.12 in Chapter 1 gives a complementary 2-D illustration of the principle. Step A in Fig.5.1 is the undisturbed part and the residual stresses that one wishes to determine. In B, the part has been cut in two on the plane x = 0 and has deformed because of the residual stresses released by the cut. In C, the deformed cut surface is forced back to its original shape and the resulting change in stress is determined. Superimposing the stress state in B with the change in stress from C gives the original residual stresses throughout the part:

$$\sigma^{A}(x,y,z) = \sigma^{B}(x,y,z) + \sigma^{C}(x,y,z) \tag{1}$$

where σ refers to the entire stress tensor and the superscripts refer to the various steps of Fig.5.1. Because σ_x, τ_{xy}, and τ_{xz} are zero on the free surface in B, the described superposition principle *uniquely* determines the original distribution of those residual stresses on the plane of the cut, i.e., at $x = 0$ in A [2].

If one could measure in-plane displacements on the cut surface, this theory would be complete. However, measurement of the transverse displacements is not experimentally possible; instead, some reasonable assumptions and approximations are required.

5.2.2 *Practical implementation*

Proper application of the superposition principle combined with a few assumptions allows one to determine the normal residual stresses experimentally along the plane of the cut: $\sigma_x^A(0,y,z)$. Experimentally, the contour (surface height map) of the free surface is measured after the cut (in B). Measurement of the surface contour provides information about the displacements in the normal (x) direction only. Therefore, the analytical approximation of Step C will elastically force the surface back to its original configuration in the x-direction only, leaving the transverse displacements unconstrained. (In a finite element (FE) model, leaving the transverse displacements unconstrained on the free surface results in automatic enforcement of the free surface conditions $\tau_{xy} = 0$ and $\tau_{xz} = 0$.) Thus, the contour method can identify the normal stresses σ_x only, and not the shear stresses τ_{xy} and τ_{xz}. In spite of the presence of any shear stresses and transverse displacements, one need only average the contours measured on the two halves of the part to determine the normal stress, σ_x. The shear stresses released on the plane of the cut affect the surface displacements anti-symmetrically. Thereby, when the average is computed, the effects of transverse displacements and shear stresses are cancelled out and the result is the surface displacements due to release of the residual stress normal to the surface [2].

Since the stresses normal to the free surfaces in B must be zero in Eq. 1, Step C by itself gives the correct stresses on the plane of the cut:

$$\begin{aligned} &\sigma_x^B(0,y,z)=0 \\ &\Rightarrow \\ &\sigma_x^A(0,y,z)=\sigma_x^C(0,y,z) \end{aligned} \quad , \tag{2}$$

which is the standard implementation of the contour method.

5.2.3 *Assumptions and Approximations*

Elastic stress release and stress free cutting process

The superposition principle assumes that the material behaves elastically during the relaxation of residual stress and that the material removal process does not introduce stresses of sufficient magnitude to affect the measured displacements. These assumptions are common to relaxation methods and have been studied extensively as described in Chapters 2 and 4 on hole drilling and incremental slitting. Plasticity errors will be discussed in more detail for the contour method later in this chapter.

Starting with flat surface in analysis

One approximation to the theory is made purely for convenience in the analysis: the deformed shape of the body is not modeled before analytically performing Step C in Fig. 5.1. Because the deformations are quite small for engineering materials, and the analysis is linear, the starting point for this step can be a flat surface and the displacement boundary conditions will then force the surface into the opposite of the measured shape. The results are the same, and the analysis is simpler.

Part is symmetric about cut plane

Averaging the contours on the two halves to remove shear stress effects requires another assumption: that the stiffness is the same on the two sides of the cut. For homogeneous materials, this assumption is certainly satisfied when a symmetric part is cut precisely in half. In practice, the part only needs to be symmetric within the region where the stiffness has a significant effect on the deformations of the cut surface, which can be estimated as extending from the cut surface by no more than 1.5 times the Saint Venant's characteristic distance. The characteristic distance is often the part thickness, but is more conservatively taken as the maximum cross-sectional dimension. If the part is asymmetric, an FE analysis can be used to estimate possible errors, which tend to be small until the part is very asymmetric.

Anti-symmetric cutting errors average away

Figure 5.2 shows that averaging the two contours removes any errors caused by anti-symmetric cutting effects – those that cause a low spot on one side and a mating high spot on the other side [10]. The two main causes of anti-symmetric errors are the cut itself wandering, as illustrated in Fig. 5.2, or the part moving during cutting as stresses are relaxed and the part deforms.

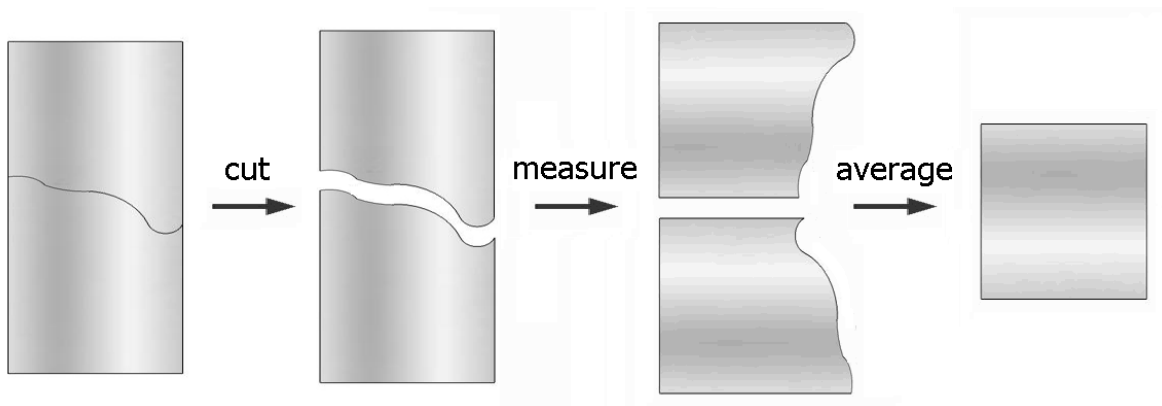

Figure 5.2. The effect of crooked cut averages away.

Symmetric errors: cutting irregularities

There are other errors that cause symmetric or asymmetric effects that do not average away. Most such error sources are relatively straightforward and can be avoided with good experimental practice. Local cutting irregularities, such as wire breakage or overburning at some foreign particle, are usually small length scale (order of wire diameter) and are removed by the data smoothing process or manually from the raw data. A change in cut width can occur in heterogeneous materials since the EDM cut width varies for different materials. A change in the part thickness (in the wire direction) can also cause this. A "bowed" cut [2,11] can usually be avoided by using good settings on the wire EDM [11].

Bulge error

It must also be assumed that the cut removes a constant width of material when measured relative to the state of the body prior to any cutting. From a theoretical point of view, the relevant assumption for the superposition principle in Fig.5.1 is that the material points on the cut surface are returned in Step C to their original locations. (The averaging of the contours on the two surfaces takes care of the issue with not returning material points to their original location in the transverse direction.)

Figure 5.3 illustrates the "bulge" error, a symmetric error that can cause bias in the contour method results [10]. The cutting process makes a cut of constant width w in the laboratory reference frame. As the machining proceeds, stresses relax and the material at the tip of the cut deforms; however, the physical cut will still be only w wide. This means that the width of material removed has been reduced when measured relative to the original state of the body. Therefore, forcing the cut surface back flat as in Step C of Fig.5.1 will not return the material to its original location, which causes an error in the stress calculation. The bulge effect is symmetric and will not be averaged away. The effect occurs when the stress state at the cut tip changes relative to the original stress state, which is caused by specimen deformation as the cut progresses. Therefore, the error can be minimized by securely clamping the part. In addition, it is worth noting that this effect scales with the width of the cut.

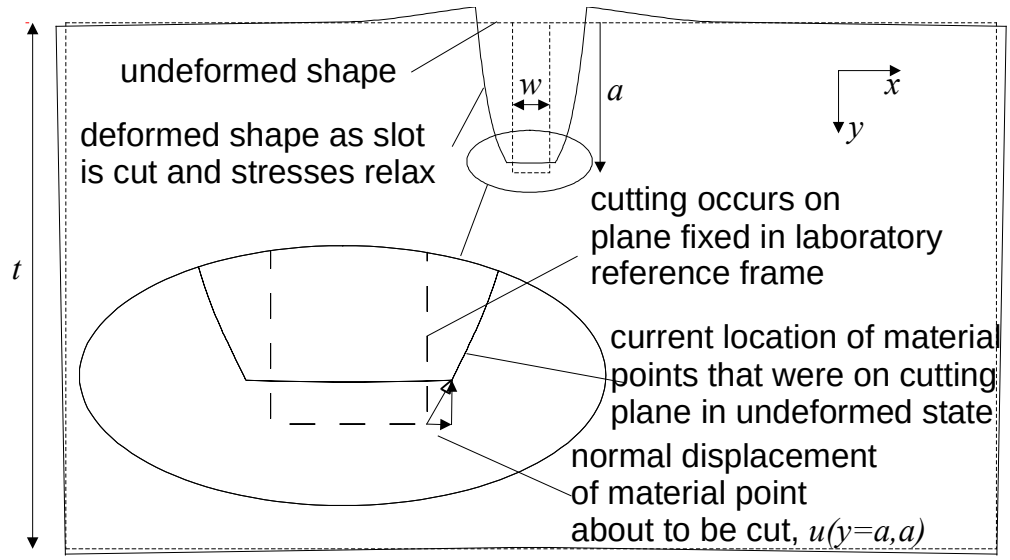

Figure 5.3. The "bulge" error occurs when the material at the cut tip deforms prior to the cut, changing the effective cut width. For simplicity, the typical round-bottomed EDM slot is illustrated as flat. From [10].

No assumptions of isotropic or homogeneous elasticity required

Bueckner's principle and the contour method do not require any assumption that the material be elastically isotropic or homogeneous, only that the linear elastic behavior be accurately reflected in the FE model used to calculate stress. Most contour method measurements assume that the material being measured is isotropic and homogeneous, which is a good assumption for many materials. However, it is possible to include anisotropic elastic constants in the material definition file and to have these constants vary spatially throughout the part. The nuclear power plant weld presented later in this chapter is an example of heterogeneous elasticity.

5.3 Practical Measurement Procedures

5.3.1 *Planning the measurement*

It is useful to spend time planning the measurement at the outset to avoid potential issues that may arise. Carefully look through the list of experimental steps and analytical steps and consider how each task will be executed. Recognize that fixturing the part and making the cut are the most important experimental aspects of the contour method, and poor technique will lead to increased errors. Measuring the surface to sufficient precision is relatively easy.

The contour method is a specialized technique that is only appropriate for particular measurements. If near-surface stresses are of primary interest consider using a different technique. Also, very small parts and or small magnitude and localized stress fields may be difficult to resolve using the contour method. In cases of concern, it is useful to simulate the experiment ahead of time.

5.3.2 *Fixturing*

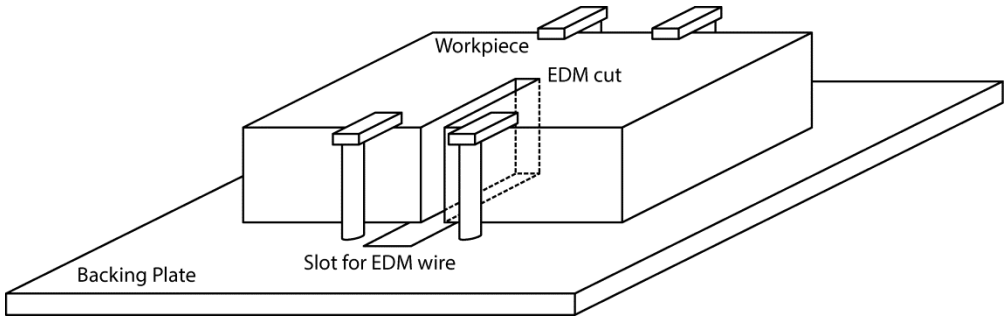

Figure 5.4. Illustration of double sided clamping arrangement used for the contour method

As discussed in Section 5.2.3, the original plane of the cut should be constrained from moving as the stresses are relaxed during cutting. Such constraint requires clamping both sides of the cut to a rigid fixture. Fig.5.4 shows an example clamping arrangement. In general, more clamping constraint is better. Care should be taken not to clamp in a manner that will induce stress into the part. Some novel approaches have been used to try to obtain maximum constraint [12,13] including self-restraint by leaving a ligament of uncut material [14,15]. Some results have been reported when the specimen was only clamped on one side [16,17], often because the same cut was used for a slitting measurement [10,18,19], which generally leads to very different contours measured on the two halves after cutting. After averaging the contours, the results are often still good, but sometimes an increased bulge error is evident [18]. In general, the use of novel fixturing arrangements should be used with great caution.

5.3.3 *Cutting the part*

For the contour method, the ideal machining process for cutting the part has the following characteristics: a straight (planar) and cut with a smooth surface, minimal cut width (kerf), not removing any further material from already cut surfaces, and not causing any plastic deformation or induce any residual stress. Wire electric discharge machining (wire EDM) is currently the method of choice. In wire EDM, a wire is electrically charged with respect to the workpiece, and spark erosion causes material removal. The cutting is noncontact, whereas conventional machining causes localized plastic deformation from the large contact forces. The part is submerged in temperature-controlled deionized water during cutting, which minimizes thermal effects. The wire control mechanisms can achieve positional precision of a fraction of a micrometer, especially for a straight cut.

Since the bulge error increases with cut width, a smaller wire diameter is recommended when possible. Too small of a wire diameter, however, will sometimes result in undesirable wire breakage during the experiment or can lead to unreasonably long cutting times. Table 5.1 shows some general guidance on minimum wire diameter relative to cut thickness. That thickness depends on the part orientation during cutting, and the orientation that minimizes thickness is generally preferred. The smallest robust wire diameter will depend on the material being cut and the EDM machine, so the table should only be used as a starting point for selecting

wire size using practice cuts. Sometimes, a larger wire size is chosen to ensure a more robust cut [11].

Specimen thickness	EDM wire diameter
< 15 mm	100 μm
10 mm – 100 mm	150-200 μm
> 50 mm	250 μm

Table 5.1. Rough guide to suggested wire sizes. The ranges overlap because the choice will also depend on the sample material and the EDM machine.

The best results have been obtained using EDM wires made of brass. Although no systematic study has been reported, the use of other wires such as tungsten or zinc-coated brass have seemed to resulted in lower quality cuts [2,20,21].

The cut quality is a primary factor in determining the quality of contour method results. In addition to selecting the proper wire size and type, it is important to select cutting conditions that produce a cut that represents, as close as possible, the conditions described above for the ideal cutting process. It is generally advisable to use a "skim" or "finish" cut setting for the machine. Skim cut settings are lower power than conventional rough cut settings (which are optimized for speed) and are intended to provide a better surface finish and minimal recast [22]. Specific cut parameters and settings are machine specific and there is typically a library of cut settings for different configurations included in the machine's control unit. Typical settings for cutting a specific material with a specific wire will include settings for a single rough cut and then for three or four sequential skim cuts. The setting for the first or second skim cut are often the best choice for the contour method, because the settings for the final skim cut often result in wire breakage or extremely slow cuts.

To cut the part, set it up on the EDM and secure it with clamps after the part and the clamps have come to thermal equilibrium with the water in the EDM tank. Align the cut path to the part and program the EDM cut to cut through the entire cross section in a single pass. Upon completion of the cut, the parts should be removed from the EDM, taking care to preserve the integrity of the cut surfaces, and rinsed to remove any loose debris that may have adhered to the surface.

5.3.4 *Measuring the surfaces*

The surfaces created by the cut should be measured. In general, the form of the surface contours will have a peak-to-valley magnitude on the order of 10 μm to 100 μm. Accurate measurement of surface height fields on this level requires precision metrology equipment. A coordinate measuring machine (CMM) is a useful and widely available device for this purpose.

The two halves created by the EDM cut should be placed on the CMM with their "cut" surfaces exposed (the term "cut" is used here to describe the surface where residual stress

measurement is performed). The metrology device should be programmed to acquire points over the entire surface with point spacing sufficient to resolve the form of the displacement field. If nothing is known ahead of time that could guide measurement density, it is possible first to measure the parts with a coarse spacing to estimate the form of the displacement field and then to measure again with a fine spacing that is sufficient to capture the necessary detail. A simple uniform grid of 50 by 50 points is a useful starting point for a CMM with a 2 mm ruby stylus. A relatively large stylus such as this is desirable because it will smooth out some of the features on the "rough" EDM surface. When possible, both surfaces should be measured using the same measurement point locations, bearing in mind that one coordinate direction will be reversed when comparing the two surfaces. Since CMM measurements occur at about one-per-second frequency, the measurements can take several hours. Therefore, temperature stability is important and the CMM should be isolated from thermal fluctuations. In addition, it is helpful for later alignment of the two surfaces to collect a series of points tracing the perimeter of each "cut" surface by placing the CMM tip slightly below the surface and touching the sides of the part. More details of CMM measurements for the contour method are reported elsewhere [23].

Other methods can be used to measure the surface, but measuring the surface contour is relatively easy and has never been the limiting factor for the contour method measurements. Non-contact optical scanners have been used widely [24,25,12] and demonstrated to give nearly identical final stress results to a CMM [26,21]. The optical scanners generally provide noisier results because they capture the roughness of the EDM cut, see Fig.5.5 for an example. Therefore, significantly denser measurement points are required. However, optical scanners can measure points more quickly, which also might reduce thermal fluctuation issues. The optical scanners generally cannot measure in the transverse direction, which means one cannot directly measure the part perimeter.

The Ph.D. dissertation by Johnson [23] gives further detailed information on measurements and analysis relating to the contour method.

5.4 Residual Stress Evaluation

In general, several steps are required to process contour data and calculate stresses. Practitioners should use care to make sure that the processed data remains as true as possible to the original data. It is suggested that intermediate results be examined carefully after each step.

5.4.1 *Basic data processing*

Align the coordinate frames

The two data surfaces, one from each side of the "cut", should be aligned to the same coordinate frame such that the material points prior to cutting are coincident on the two surfaces. The two cut surfaces appear as mirror images, so one of the Cartesian coordinate directions needs to be reversed so as to connect corresponding points on the two surfaces. This coordinate reversal can be seen in the third panel of Fig.5.2, when the lower section has been reversed to register with the surface of the upper section. If further alignment is required then it is necessary to perform rigid body translations and rotation in the plane of the cut surface to set both surfaces in the same coordinate frame. For example, if the measured surface is approximately oriented in the *yz*-plane then it is necessary to translate one surface in *y* and *z* and also rotate it about the *x*-axis until it sits on top of the other surface (when viewed along the *x*-axis). The perimeter trace

is very useful for this alignment. The other rigid body translation (x-direction) and rotations (about y and z) will not affect the results and can be ignored. It is generally convenient, however, to fit each surface to a best fit yz-plane and to subtract this from the data (which will bring each surface close to the yz-plane).

Following surface alignment, the perimeter trace should be decoupled from the data sets. The perimeter trace may be used to support FE model construction and after that it is no longer needed.

Construction of FE model

A finite element model representing half of the original part, e.g., the shape of one of the two pieces after it has been cut in half, should be constructed based upon measurements of the part. If available, the perimeter trace of the cross-section from a CMM represents a useful starting point for the model. If the cross-section is relatively simple, then measurements using a linear measurement tool such as calipers provide a useful alternative. This cross section can typically be "extruded" in the third dimension based on simple dimensional measurements. The finite element model should represent the cross-section of the part at the measurement plane and should have a similar stiffness relative to displacements being applied on the measurement surface. Features in the part "far" from the measurement plane are unlikely to influence this stiffness and can typically be ignored.

A finite element mesh should be generated on the model. It is useful to bias the mesh for higher refinement near high gradients in the displacement surface and near edges of the measurement cross section. This can help to produce a converged solution in an efficient manner. First order hexahedral (brick) elements or second-order reduced-integration hexahedra are preferred. A useful starting point for the mesh density is 50 by 50 elements over the cross section. The element size can be relaxed to grow large away from the measurement plane without affecting the stress results. Figure 5.6 later in this chapter shows an example.

Once complete, a list of nodes on the cut surface where displacement boundary conditions will be applied should be generated along with their coordinates. This list will be used to generate prescribed displacement boundary conditions.

Average the two sides

Once the two surfaces are aligned, the data from both surfaces should be averaged. This can be accomplished by taking the matching points from each surface and computing the average value.

Filter the noise

The surface measurement data will contain some "noise" that is the result of measurement error and roughness on the EDM cut surface. The random noise and roughness are not caused by bulk residual stresses, however, they will significantly affect the calculated stress because the stress depends on the curvature of the displacement field and this high frequency content has a high curvature. For this reason, it is important to remove the noise from the data while preserving the overall form of the surface (which is the result of bulk residual stress).

A two-step process can be used to prepare the displacement data for stress computation. First, obvious outliers should be deleted from the data set. Outliers can result from unintended particles such as dust settling on the surface during measurement, artifacts from measurements

near the edges of the perimeter, and gross measurement errors. Outliers can be identified by plotting the data surface and visually looking for points that are significantly away from the overall form of the surface.

Second, a method should be employed to extract the form of the surface while eliminating the roughness and noise. This is typically accomplished by fitting the data to a smooth surface (e.g., bivariate splines). There are commercial software packages available for straightforward implementation of this including MATLAB® which has a Spline Toolbox®. Spline smoothing has been most widely used [26] but in most formulations requires that the data points be on a regular, rectangular grid, which can require extra processing to grid the data. Alternately, the data can be fit to a continuously defined smooth surface, such as a bivariate Fourier series, without gridding the data [27,28]. A continuous surface sometimes cannot fit the data as well as local splines. A few alternative approaches for smoothing the data have also been reported in the literature [29,30,18]. Any method that filters the surface roughness while accurately capturing the overall form of the contour should be acceptable.

There is not yet a robust, objective method for selecting the optimal amount of smoothing. Examining plots of the misfit, the difference between the experimental displacements and the fit, is very helpful [23]. Often, the fit is selected using a linear or semi-log plot of the root mean square (RMS) misfit versus increasing spline knot density or order of series fit. The fit where the RMS misfit begins to flatten out is selected because it often represents the transition point between over-fitting and under-fitting the important features of the data [26,24,31]. Improved selection of smoothing might be possible by estimating the uncertainty in the stresses and picking the fit that minimizes the uncertainty [26].

Transfer to FEM

The final displacements, after averaging and filtering, should be inverted about the surface normal and interpolated/extrapolated to the node locations on the finite element surface as displacement boundary conditions. Only the displacement in the direction normal to the surface of the cut should be specified, and it must be specified for all nodes on the cut surface. Three additional point boundary conditions should be applied to the model to restrain rigid-body motion (but nothing more). Such a minimal constraint arrangement ensures that the calculated residual stress map satisfies equilibrium, and is the reason that rigid body motions of the measured contour do not affect the results. Figure 5.6 shows an example with the following rigid-body motions being constrained: translation in y and z and rotation about the x-axis. Once the boundary conditions are in place, the model should be allowed to reach equilibrium. The resulting stresses on the plane of the cut in the normal direction are the "results" from the contour measurement. These represent the original residual stresses in the part prior to sectioning.

Reporting results

Practitioners should report sufficient details so that an expert reader can independently interpret the results. Descriptions of the part's material should be detailed and include the heat treatment state and the yield strength. The arrangement used to clamp the part during cutting should be illustrated or described. Description of cutting should include the EDM wire diameter and material, the cut settings, the rate of cut, and any wire breakages or other issues. Description of the surface contouring should include the instrument details, the measurement density, and the thermal conditions throughout the measurement duration. The resulting surface contour maps

should be plotted or described including the peak-to-valley range of each side. The sequence of steps used to process the data should be described in detail. Ideally, the smoothed surface contour should be plotted as should the misfit between the data and the smooth surface. The misfit should be quantified as a root-mean-square average. The description of the FE calculation should include mesh and element details. Stresses near the perimeter of the measurement surface may exhibit higher measurement uncertainty than points in the interior, see Section 5.6.1 . Typically, some data near the perimeter are discarded before plotting.

5.4.2 *Additional issues*

Order of data processing steps

The outline of experimental steps presented above is considered to be a straightforward approach to performing contour method measurements. In practice, the order of data processing steps in going from raw displacement measurements to transferring the displacements to the FEM can vary significantly while still achieving satisfactory results. For instance, the data averaging described above assumes that both sets of data contain points at the same location. This is not always the case. If the sets of surface points do not match, then it is necessary to interpolate them onto a common set of points before averaging. The set of common points could be one of the data surfaces, a regular grid, or the finite element node locations. As an alternative to interpolating onto a grid for averaging, one could smooth each surface independently and then average the smooth surfaces.

Extrapolation

Displacements must be defined on all nodes on the cut surface in the finite element model. Because of finite distance between measurement points, part alignment and other experimental issues, the data generally will not extend all the way to the perimeter of the surface. In some way, the displacements must be extrapolated to the perimeter, but the method will depend on other data processing choices. If gridded or otherwise regular, the data can be linearly extrapolated out to the edges [23,32]. Alternatively, the smoothed surface fitted to the data can be used to extrapolate to the perimeter, but then the choice of fit surface can have a strong effect on the extrapolation [18]. Any region where the data were extrapolated should be considered unreliable and the stresses there not reported in the final results.

No filtering

With careful planning, it can be possible to perform a measurement without any post-measurement filtering of the displacement data [12,33]. If the finite element node points are known prior to performing the surface displacement measurements then the CMM can be programmed to take displacement measurements directly at these locations. For this to work effectively, the raw displacement data should be as smooth as possible, for example, using a large measurement stylus and averaging multiple measurement values. These displacement data can then be directly averaged and applied to the finite element model. If carefully implemented, this approach can result in stresses that are reasonably smooth. If necessary, the computed stresses can be smoothed at the end of the analysis.

Stress-free test cut

It is good practice to verify the cutting assumptions by performing a similar cut on a part with the same cross-section in the absence of residual stress [10,11]. Since stress-free material

can be difficult to find, such a test is often performed by cutting a slice off of the end of the part. That region is nearly stress-free because of the adjacent free surface. The thin slice will often have unrepresentative deformations, but the cut surface on the larger piece can be examined. Displacements measured on the test cut surface should not have significant form, i.e., the surface should be flat. In some reported cases, the experimental displacement data have been "corrected" based on the form observed in the stress-free cutting condition [2,34,20]. A brief example of this is discussed later in the experimental application of the stainless steel indented disk.

5.5 Example applications

5.5.1 *Experimental validation and verification*

This section presents experimental applications of the contour method where there are independent residual stress measurements for comparison. The first example compares with neutron diffraction and is from a class of specimens that tends to provide good agreement with neutron diffraction: non-welds. The second example is a linear friction weld with very high stress magnitudes and gradients, also compared with neutron diffraction. The third example is a laser peened plate with near surface stress gradients, compared with incremental slitting and x-ray diffraction with layer removal.

There are currently approximately two dozen published comparisons of contour method measurements with other measurements, primarily neutron and synchrotron diffraction, but also some relaxation methods. Such independent validations commonly show very good agreement on non-welded specimens [2,35,36,20,37-39] and on friction welded specimens [40,41,23], but not always [30,21]. Fusion welds sometimes showed good to very good agreement [42,26,29,43,28,44,19,18,45] and sometimes noticeable disagreement in some regions [46-50]. It is difficult to assess which results are more accurate when the two methods disagree. Welds are challenging for diffraction methods because of spatial variation of the unstressed lattice spacing and because of intergranular effects (microstresses and strains), as discussed in Chapters 7 and 8. Welds can also be challenging for contour measurements because the stresses can be quite high and the local yield strength may be lowered by the thermal process, both effects increasing plasticity errors. In addition, some of the measurements reported in the literature (both neutron and contour) were not done using the best practices.

Indented stainless steel disk compared with neutron diffraction

This example is presented in Chapter 8 on Neutron Diffraction with additional details. 60 mm diameter, 10 mm thick disks of 316L stainless steel were plastically compressed through the thickness with opposing 15 mm diameter, flat-end, hard steel indenters in the center of the disk [20], as illustrated in Figure 8.7 . The residual hoop stresses on a diametrical plane of two disks indented under the same experimental conditions were measured with the contour method, see Fig.8.9. Disk A was cut in half using wire EDM with a 50 μm diameter tungsten wire. To avoid repetition of errors attributed to that wire, disk B was cut using a 100 μm diameter brass wire. As controls, two stress-free unindented disks were also cut using the 50 μm and 100 μm diameter wires, respectively.

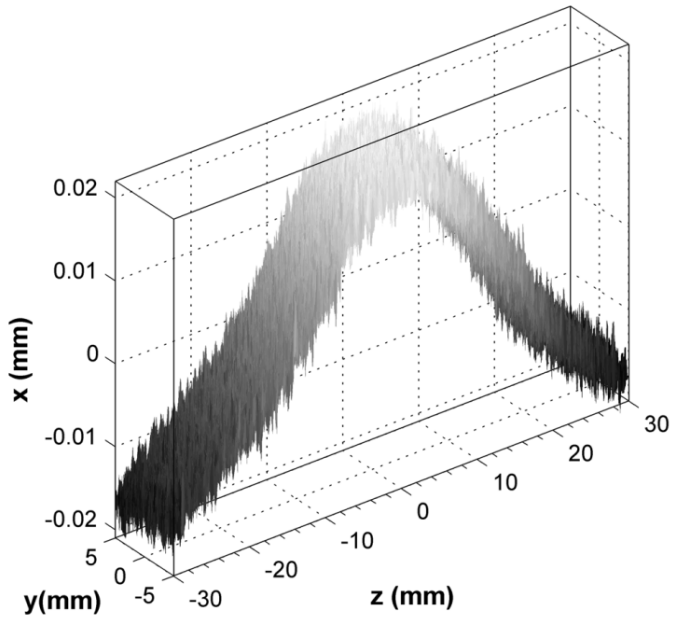

Figure 5.5.The average measured surface contour on one of the disks. From [32]

The contours of both cut surfaces of each disk were measured using a laser scanner [26]. For disk B, Fig. 5.5 shows the average measured contour. The peak-to-valley amplitude of the contour is about 40 μm. The surface roughness level in the measured contour is typical of laser scanners and much larger than what is measured using a CMM with a spherical tip. The cut surfaces of the two stress-free, unindented disks were also measured. The contour of the disk that was cut using the 100 μm brass wire was flat to within the measurement resolution. The contour of the disk that was cut using the 50 μm tungsten wire was bowed: higher by about 6 μm on the top and bottom edges of the 10 mm thickness than in the mid-plane. In order to correct this effect, the contour on the unindented disk was subtracted from the contour of the indented disk A, which was cut with the same wire.

Figure 5.6 shows the finite element model used to calculate the residual stresses. The mesh for the half-disk used 51,920 linear hexahedral 8-node elements with reduced integration (C3D8R). The material behavior was considered elastically isotropic with an elastic modulus of 193 GPa and a Poisson's ratio of 0.3. To avoid clutter in the figure, only two typical displacement boundary conditions are illustrated, but all nodes on the cut surface had *x*-direction conditions applied.

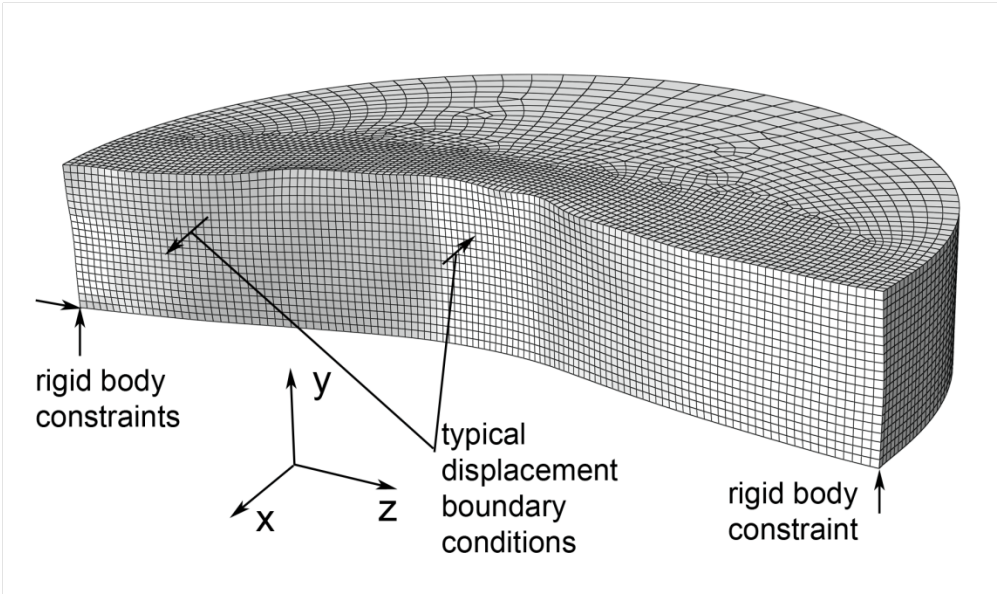

Figure 5.6. Finite element mesh of half-disk after displacement boundary conditions have deformed the cut surface into the opposite of the measured contour. Deformations exaggerated by a factor of 200.

Figure 5.7 shows the contour-method maps of residual hoop stress on the cross sections of the disks. In spite of the correction required on the Disk A data, the results agree to within about 20 MPa over most of the cross section. The contour results are compared to extensive neutron diffraction measurements on the same disk in Fig. 8.10 in Chapter 8. The agreement between the contour method and neutron diffraction is excellent. Note that the contour results have a mild left-right asymmetry even through the specimens were prepared to be as axisymmetric as possible. The asymmetry probably reflects a slight bulge error as discussed in Section 5.2.3 .

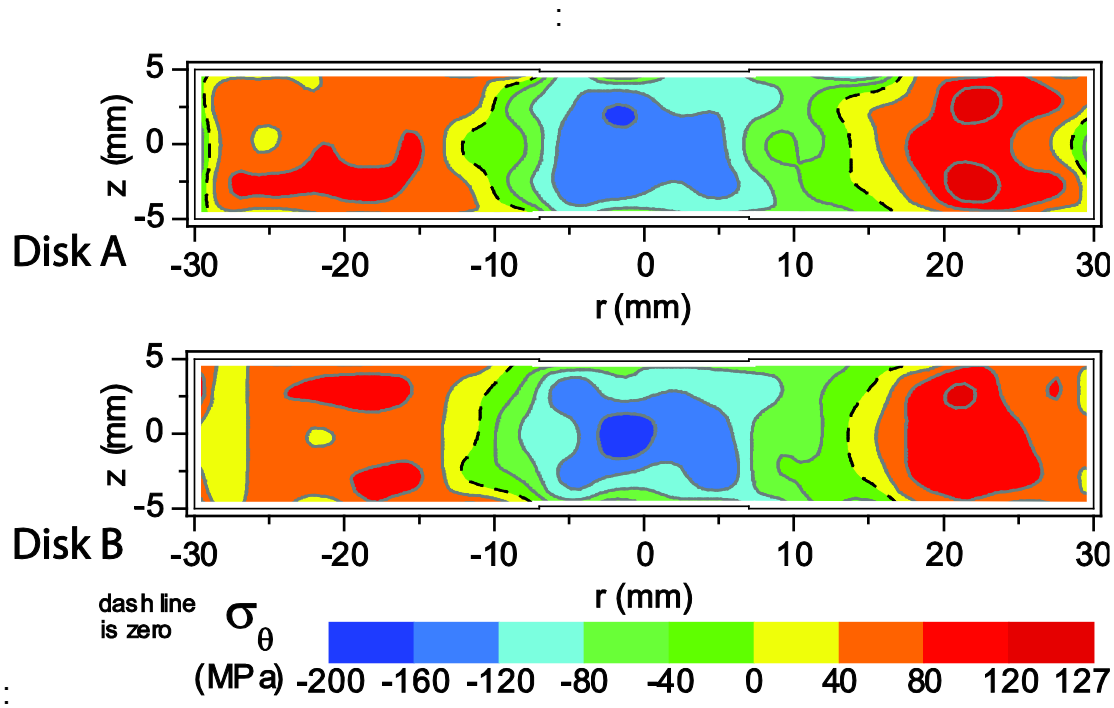

Figure 5.7. Hoop stresses measured on cross section of indented steel disks. The results agree very well with neutron measurements as shown in Figure 8.10. From [20].

Linear friction weld compared with neutron diffraction [51]

Sample blocks 38.1 mm tall by 50.8 mm wide by 12.7 mm thick machined from Ti-6Al-4V alloy bar stock were joined (at the 50.8 mm by 12.7 mm face) using linear friction welding (Fig. 5.8). The LFW process produces a narrow bond region and heat affected zone where the microstructure is altered from its original condition. Residual stresses were measured in the LFW test specimen using the contour method and neutron diffraction. The measurements were performed on the same test specimen, in sequence. First, neutron diffraction was used to measure σ_x, σ_y, and σ_z along the line through the center of the specimen shown in Fig. 5.8. Following completion of the neutron diffraction measurement, the contour method was used to measure σ_y over the plane shown in Fig. 5.8.

Figure 5.9 shows a plot of the two dimensional residual stress measured using the contour method. There is a concentrated region of high-magnitude tensile residual stress near the LFW joint. The peak stress magnitude is around 750 MPa. The tensile stress quickly diminishes to slight compression away from the LFW joint.

Data were extracted from the 2D contour surface along the same line where the neutron diffraction measurements were performed, and the comparison is plotted Fig. 5.10. Overall, there is very good correlation between the two measurement techniques. The neutron diffraction data show slightly higher magnitude peak stress at the center of the weld (nominally 800 MPa versus 750 MPa, which is a 6% difference). The width of the tensile stress region is very similar for both sets of measurements. Since the results in Fig. 5.10 differ by an almost constant shift of about 50 MPa, the most likely explanation for the modest differences between the two

techniques would be an error in the unstressed lattice spacing used for the neutron stress determination.

The peak stress magnitudes are large, which makes plasticity a potential issue for the contour method measurement, but the agreement with neutron results indicate that plasticity was not a significant problem. The yield strength of the Ti-6Al-4V prior to welding was about 915 MPa. The occurrence of yielding during a contour measurement is a complicated phenomenon that depends on the full multiaxial stress state, the prior thermal and plastic history of the material, and the effectiveness of the part clamping. This LFW example should demonstrate that the contour method can at least sometimes get accurate results even with very high stresses.

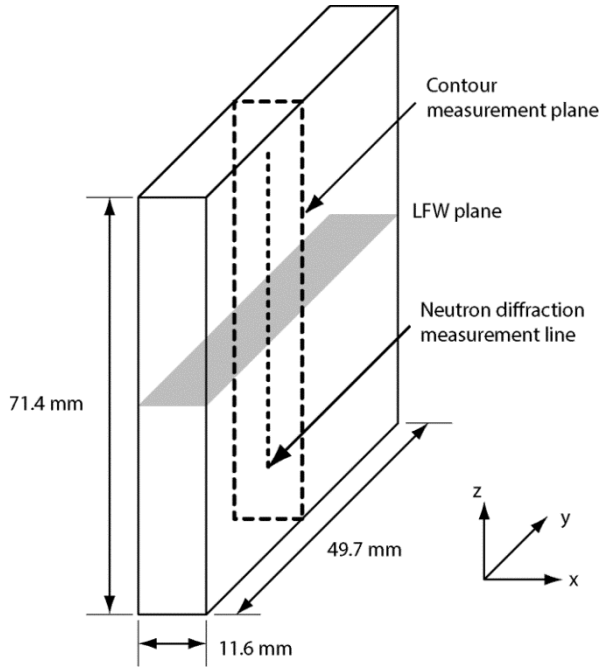

Figure 5.8. Illustration of LFW test specimen showing dimensions, reference coordinate frame, and measurement locations. From [51]

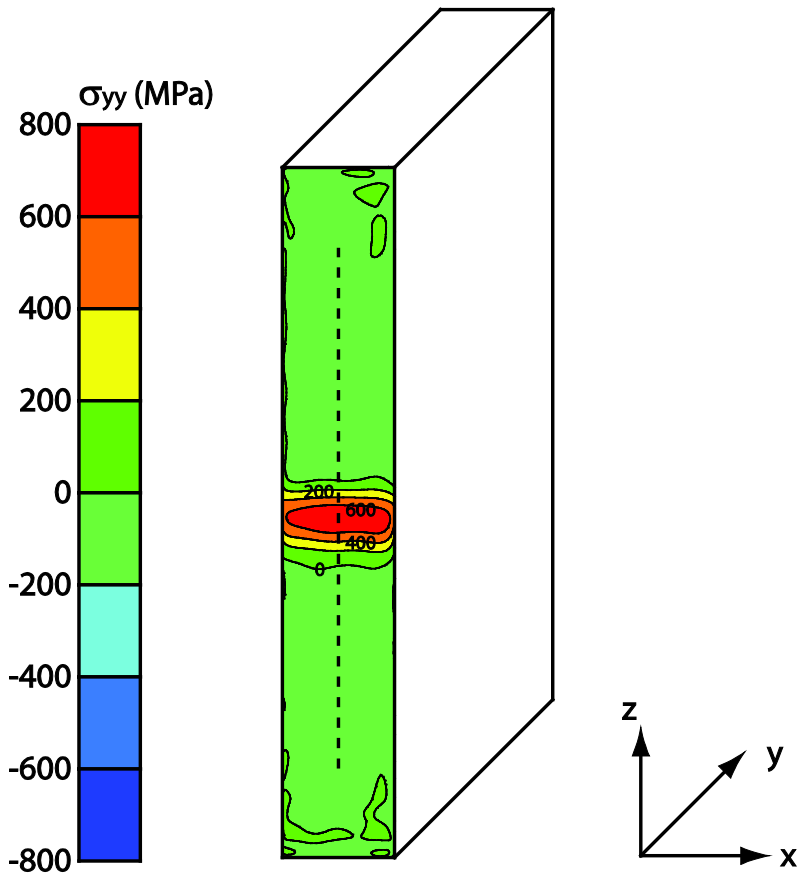

Figure 5.9. Two-dimensional map of the measured residual stress over the contour measurement plane. From [51].

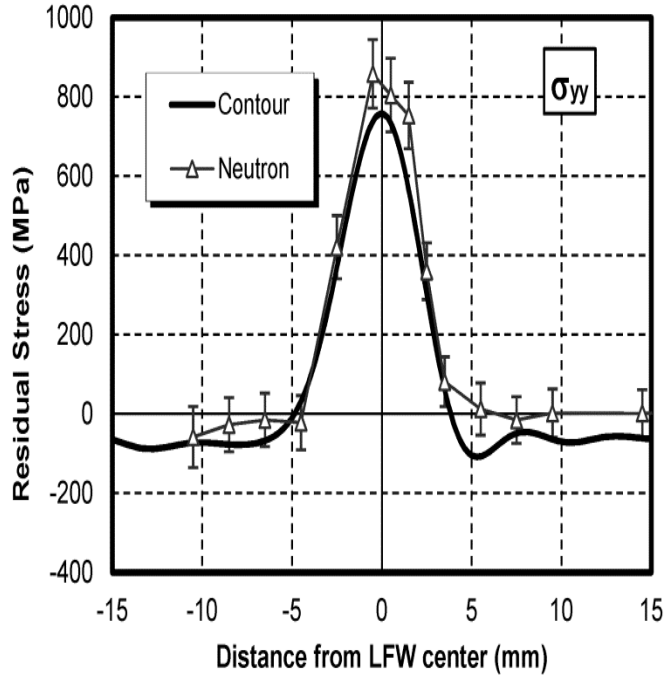

Figure 5.10. Line plot comparing the measured residual stress from the contour method and neutron diffraction experiments. From [51].

Laser peened plate compared with slitting and X-ray diffraction with layer removal

A plate of Ti-6Al-4V with original dimensions of 50 mm x 50 mm x 8.7 mm, shown in Fig.5.11, was processed using laser shock peening (LSP) over the top surface to induce a uniform layer of compressive residual stress. The plate was then cut into four equal size blocks, each nominally 25 mm x 25 mm x 8.7 mm) which are expected to contain similar amounts of residual stress. Residual stress measurements were performed on three of the four blocks using different techniques: the contour method, the slitting method, and x-ray diffraction with layer removal.

Figure 5.12 shows a two-dimensional map of the residual stress in the block measured using the contour method. As expected, the block has compressive residual stress near the laser peened face, which transitions to tensile stress near the interior, and then back to compressive residual stress on the back face. The tensile residual stress in the interior and the compressive stress on the back face are the results of the plate reacting to the strain induced by laser shock peening to achieve an equilibrium stress state. A line plot of residual stress versus depth at the center of the block is shown for the contour method, the slitting method, and x-ray diffraction with layer removal in Fig. 5.13.

Overall there is excellent agreement between each of the three residual stress measurement techniques. The most significant differences are in the near surface region at depths less than 0.5 mm) but even at these locations the differences are relatively small, generally 10% and up to 20% in the extreme case.

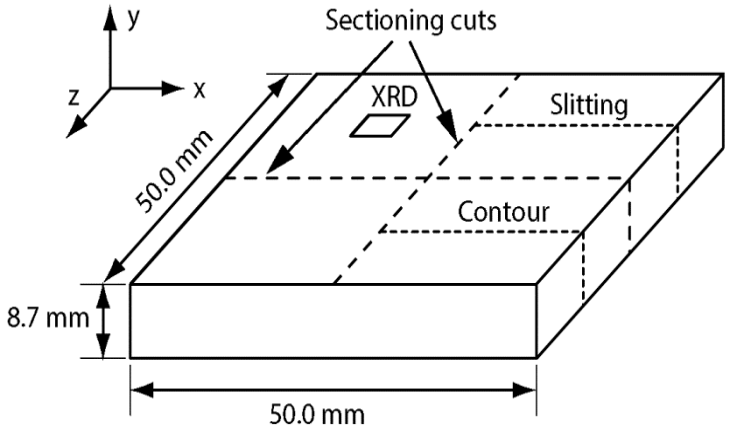

Figure 5.11. Illustration of laser shock processed test specimen used for residual stress measurement

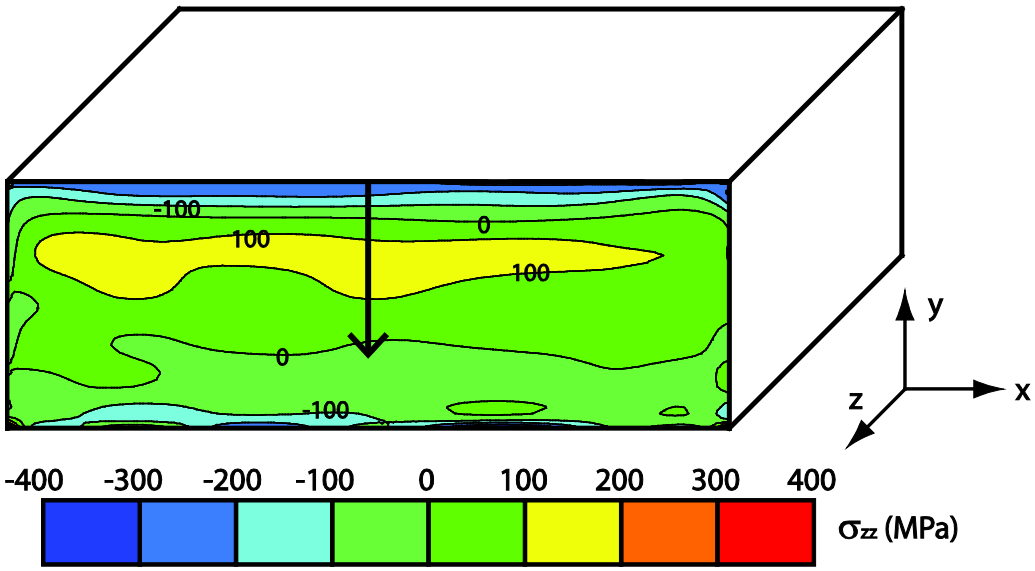

Figure 5.12. Two-dimensional map of the measured residual stress using the contour method

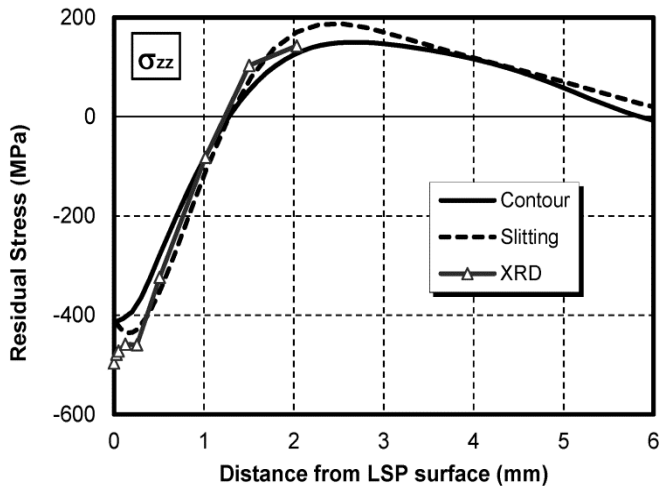

Figure 5.13. Line plot of residual stress vs. distance from the surface in a laser shock peened Ti-6Al-4V block measured using contour, slitting, and x-ray diffraction with layer removal.

5.5.2 *Unique measurements*

This section presents experimental applications of the contour method that exemplify some of the unique capabilities of the technique. The first example is a very large and complicated weld joint taken from a nuclear power plant. The second example is railroad rails that show a very informative 2D distribution of stresses. In both of these examples, largely because of their size, there is essentially no other way to measure the 2D stress maps that contour provides.

Large dissimilar metal weld from a nuclear power plant [52]

A contour method measurement was performed on a relief nozzle from the pressurizer of a canceled nuclear power plant. The nozzle was nominally 711 mm long with a 201 mm outer diameter and an inner diameter of 113 mm and contained a nickel based dissimilar metal weld used to join a carbon steel component to stainless steel piping, see Fig. 5.14. Dissimilar metal welds are particularly susceptible to primary water stress corrosion cracking and residual stresses can have a significant influence on this failure mode.

As part of this study, the contour method was used to measure residual stress at six locations in two similar nozzles. Only a single measurement is included here due to space limitations, a two-dimensional map of the hoop residual stress in the nozzle. To facilitate measurement, the nozzle was first instrumented with strain gages and cut open to relieve the bending moment in the hoop direction. The residual stress released from this process was accounted for in the results using a finite element based approximation. Next, the contour method measurement was cut opposite the initial cut. Cutting was performed using 0.25 mm diameter brass wire.

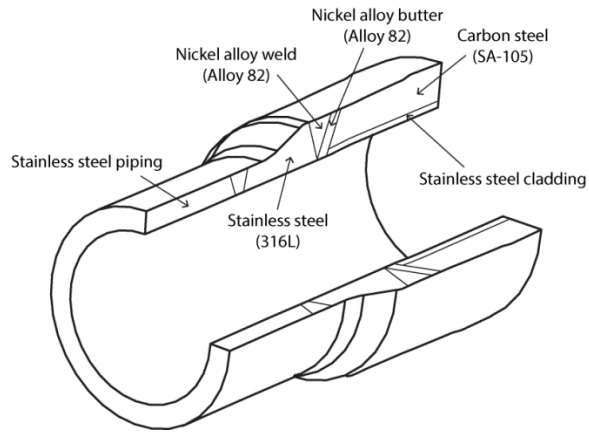

Figure 5.14. Illustration of nozzle specimens used for residual stress measurement.

To account for the different materials, regions of the finite element model were assigned elastic properties unique to each material. Figure 5.15 shows a contour plot of the measured hoop residual stress in the nozzle. Significant compressive hoop residual stress exists on the inner diameter near the dissimilar metal weld. The region of compressive hoop residual stress grows larger through the Alloy 82 "butter" and into the carbon steel region. Compressive stresses by the ID are not likely to cause stress corrosion cracking, so are an encouraging result. However, weld repairs are not present in this nozzle, and have been shown by others to produce high residual stress on the ID, which could be problematic. Tensile hoop residual stress exists near the outer diameter, in a region that is shifted towards the stainless steel end of the nozzle.

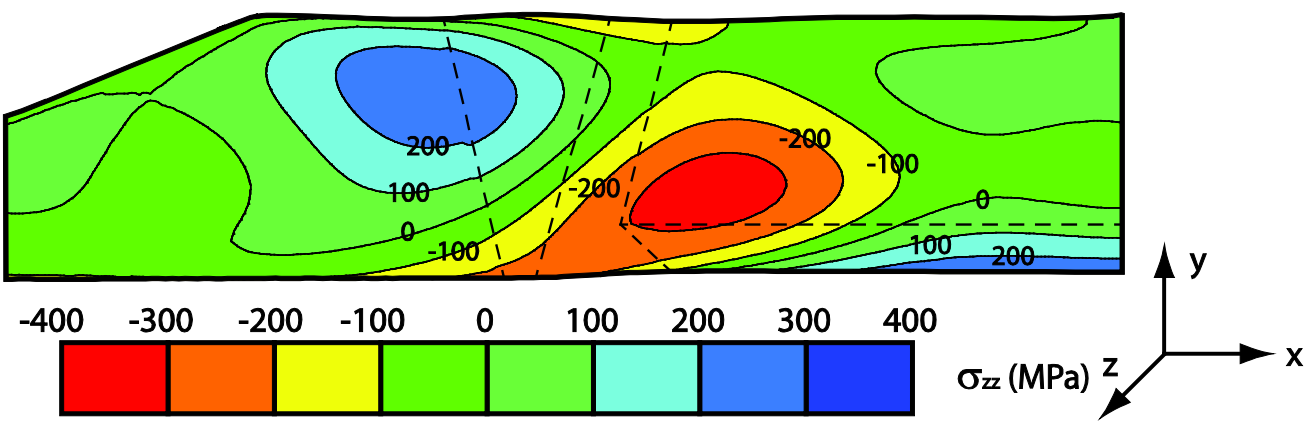

Figure 5.15. Two-dimensional map of the hoop residual stress for Nozzle #3 160-deg location. From [52].

Railroad rail

For a study motivated by the 2000 fatal rail accident at Hatfield, UK, longitudinal residual stresses were mapped in two specimens of UK rail: a new roller-straightened rail and one that had undergone 23 years of service [53]. Both rails were BS 11 normal grade pearlitic steel with the standard 113A profile, and 76 cm long sections were measured. The sections were clamped securely and cut in two using EDM and a 0.25 mm diameter brass wire. The surfaces were then contoured by scanning with a Keyence LT-8105 confocal ranging probe, similar to the

procedure described in [26]. The surface was scanned in the horizontal direction (x in Fig. 5.16) at a sampling rate of 16 points/mm, and the rows were spaced vertically to give 4 rows per mm. This produced about 460,000 points on each surface. The peak-to-valley range of the contours was about 75 μm. The data points were interpolated onto a common grid mimicking the original data grid. A rectangular region that covered the entire cross-section was defined and then regions with missing data were filled in by extrapolation. At each grid location over the rectangle, the two data points were then averaged. This average point cloud was then fit to a smooth surface using bivariate (tensor product) cubic smoothing splines [26]. The stresses were calculated by forcing the cut surface, taken as initially flat, into the opposite shape of the measured contour in a 3-D, elastic, FE analysis.

The resulting stress maps shown in Fig. 5.16 were especially informative. The new rail shows a complicated stress pattern associated with plastic deformation from the roller straightening process [54]. The residual stresses are tensile in the head and foot of the rail, with the peak stresses located subsurface. There are balancing compressive stresses in the web and in the lateral regions of the foot. The worn rail results show that the stresses changed significantly. The stresses have become significantly compressive under the region of contact with the wheel, as had been observed previously with other techniques. The contour maps, though, show other changes that have never been experimentally observed before. The tensile stresses have increased in the subsurface region of the head in a matter consistent with plastic flow driven by the angled wheel contact. Subsurface initiated cracks in this region cause failures and a significant portion of train derailments occur because subsurface cracks are hard to detect. The contour results also show an increase in the magnitude of compressive stresses in the lateral region of the foot, which may be caused by plastic deformation since the rails are known to reduce in height over time.

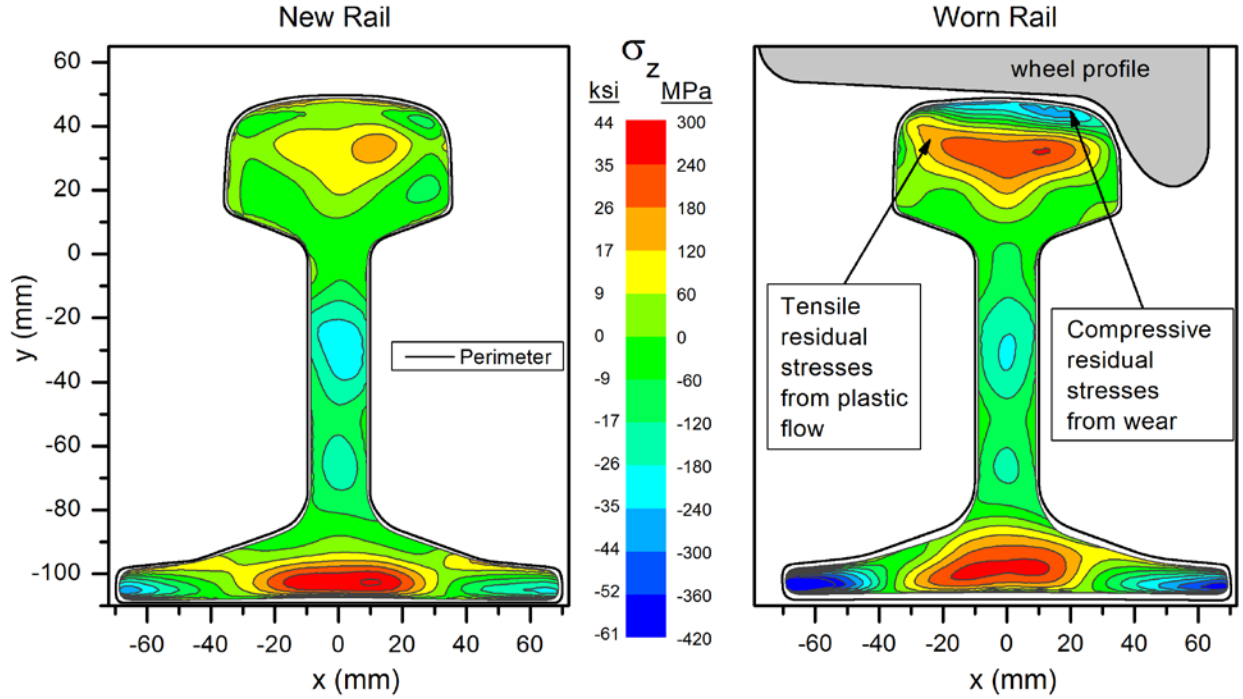

Figure 5.16. Contour method maps of longitudinal residual stresses in UK rails show the effects of roller straightening on the stresses in a new rail and the extensive effects of wear and plastic deformation on the stresses in a worn rail.

5.6 Performance and Limitations of Methods

The contour method is nearly unique in its ability to measure a 2-D cross-sectional map of residual stresses in even large parts. When used correctly and on appropriate specimens, the results are reasonably accurate and reliable. Based on all of the validations in the published literature, accuracies and uncertainties in the best test conditions can be estimated to be as low as the larger of about 10% or $\sigma/E \approx 0.00015$ (30 MPa in steel or 10 MPa in Aluminum – but these numbers really depend on part size as discussed below). Several publications demonstrate that the contour method is also repeatable to these levels or better [27,55,56,20,33]. When selecting a measurement technique for stress distributions that are primarily 1-dimensional, better accuracy can likely be achieved with other methods, like incremental slitting. To date, the contour method has only been applied using wire EDM to make the cut, which limits the application to metals and a few other materials that can be cut with EDM.

The remainder of this section discusses the conditions under which one can or cannot achieve the best results.

5.6.1 *Near surface (edge) uncertainties*

Stresses near the perimeter of the measurement surface may exhibit higher measurement uncertainty than points in the interior depending on the nature of the stress field and the details of the surface displacement measurement and data processing. Furthermore, the assumption of constant cut width may be less accurate near the edges of the cut surface. For example, the EDM

cut width may flare out a little bit at the top and bottom of the cut (entry and exit of the wire) or at the beginning or end of the cut [11,10]. Also the surface height map can be uncertain because, especially with noncontact scanners, it can be difficult to know exactly where the edge of the surface is and accurately determine the surface height. Contour method results can therefore be more uncertain near the edges of the cut. Depending on cut quality and measurement details, the uncertain region is typically about 0.5 mm. With special care, good results have been achieved closer to the edges [23,35,56]. Results should not be reported in the near-surface region unless such special care has been taken. Recently, an improvement in cut quality at the exit edge of the EDM wire has been achieved by using a sacrificial layer attached to the part surface [11].

5.6.2 *Size dependence*

The contour method generally works better on larger parts. Other relaxation methods for measuring residual stress, e.g., hole drilling and slitting, tend to be relatively size independent because, for a given stress magnitude, measured strains do not change when the part size is scaled up or down. Rather than strain, the contour method measures the surface shape, to infer displacements. For a given stress distribution, those displacements scale linearly with the part size. The EDM surface roughness and other cutting artifacts tend to remain relatively fixed in magnitude. Therefore, larger parts give more easily measured contours than smaller parts when all else is equal.

With current technology, a minimum peak-to-valley surface contour of 10-20 μm is suggested in order to get reasonable results. If one has an idea of stresses, the expected contour can be estimated prior to the experiment with an elastic FE model. The smallest parts measured with the contour method have been about 2-6 mm thick [17,57,38,55,16,58,43,35,25,59-61,24], and in some of those cases the contour is averaged over the thin dimension resulting in a 1-D profile of the stress averaged through the thickness. The main limitation to achieving good results with smaller parts [62] and smaller contours than about 10 μm is the cut and surface roughness quality currently achievable with EDM, which degrades the signal-to-noise ratio of the measured displacements. Measuring the surface contour is relatively easy and has never been the limiting factor for the contour method measurements.

5.6.3 *Systematic errors*

Bulge

The bulge error (illustrated in Fig. 5.3) results from elastic deformation and can be estimated using an FE model and even corrected for [10]. However, the error varies along the length of the cut tip, requiring a 3D model in the general case, depends on the circular shape of the cut tip, and must be estimated at incremental cut depths. Therefore, an FE estimate can be tedious. Figure 5.17 shows a 2D FE-based correction of the bulge error for a plastically bent beam [10,2]. The bulge effect estimated in Fig. 5.17 is qualitatively typical of what can be expected: a reduction in the peak stress and a slight shift of the peaks. The error depends on the cut direction. Some results in the literature [28,48], especially those were the specimen was clamped on only one side [19,10,16], show indications of possible bulge errors.

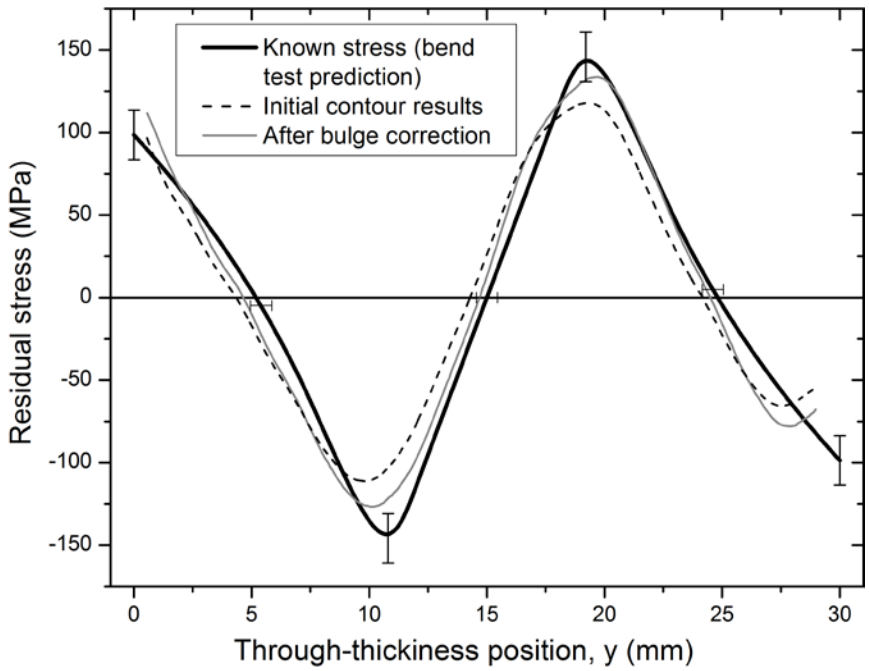

Figure 5.17. The bulge error in a plastically bent beam had a modest effect on the residual stress profile. From [10].

Plasticity

Like all relaxation methods, the contour method requires the assumption that as residual stresses are released, the material unloads elastically. The stress concentration at the cut tip may cause local yielding, which can affect the measured contour and therefore cause errors. The plasticity error is even more difficult to simulate than the bulge error, because in addition to needing a 3D model of many cut increments, it is also necessary to simulate reverse yielding behavior accurately. Only two studies of the plasticity effect are presently published in the literature. A simplistic 2D FE parameter study indicated relatively low plasticity errors for the contour method even with residual stresses at 70% or more of the yield strength [63]. A more sophisticated model indicated large errors for a particular specimen but started with residual stresses well above the yield strength [64]. In general, plasticity errors are mitigated by the round EDM cut tip and by strain hardening in the material. It is difficult to make any general statements about the sensitivity of the contour method to plasticity errors. Some contour method measurements have returned very high residual stresses but agreed well with diffraction measurements, indicating minimal plasticity errors [18,26,65,20,19]. There are also many examples were the agreement is not as good [30,48,50,49], and some of those likely have plasticity errors, but they are usually welds and it is sometimes difficult to assess the accuracy of the diffraction measurements used for validation.

For three reasons, it can be very misleading to compare measured residual stress magnitudes to the yield strength when assessing the potential for plasticity. First, the yield strength values usually reported are those of the as-received material. Often the same processes that produce the residual stress also change the yield strength, increasing it by strain hardening or decreasing it by thermal processes, which can significantly change the propensity for yielding

and errors. Second, the measured residual stress values are generally for a single stress component, but a von Mises effective stress is what should be compared with the yield strength. Peak residual stresses are often in a region of high triaxialty, which makes the effective stress lower than the peak individual stress component. Third, cut tip yielding is driven by the integrated effect of all the released residual stresses, which can be characterized by the intensity factor, K_{Irs}, at the cut tip from the accumulated effect of releasing residual stress. As studied for the slitting method, the total effect will depend on the distribution of stresses rather than just the peak stress and can be low since residual stresses must satisfy force equilibrium and therefore compressive regions tend to mitigate tensile regions in the integrated effect [66].

5.7 Further reading on advanced contour method topics

5.7.1 *Superposition for additional stresses*

The conventional contour method measures one stress component. There are two more advanced implementations where the contour method can be used to measure multiple stress components by using superposition of multiple measurements, each validated by comparison with neutron diffraction [32,37]. To explain the superposition methods, observe that Equation (2 in this chapter came from applying Equation 1 to a location, specifically the cut surface x=0, where $\sigma_x^B = 0$. For other stress components and/or other locations, the σ^B stresses can be measured. In the "multiple cuts" method [32] a second cut is made to measure stresses on a new cut plane with the contour method. Such stresses would have been affected by the first cut, but the contour measurement and calculation for the first cut also determines the change in stress on the location of the second cut (and elsewhere). For the example of a second cut to measure σ_z on the plane at $z = 0$ in Fig. 5.1, the original σ_z stresses are given by

$$\sigma_z^A(x,y,0) = \sigma_z^B(x,y,0) + \sigma_z^C(x,y,0) \tag{3}$$

where the σ_z^B term is the contour method result from the second cut and σ_z^C over the plane of the second cut is just σ_z on that plane extracted directly from the same FEM calculation used to determine σ_x for the first contour cut. Because this method is very new, there are few examples in the literature [11,67], including one using the slitting method instead of contour [68]. In previous work with multiple cuts, the correction was not made to account for the effects of previous cuts [69].

The second superposition method involves using multiple methods instead of multiple cuts [37]. For example, the in-plane stresses *on the cut surface* ($x = 0$) in Fig. 5.1 could be measured using x-ray diffraction or hole drilling once the EDM-affected layer is removed by electropolishing. For the example of σ_z, the original residual stresses on the cut plane are given by

$$\sigma_z^A(0,y,z) = \sigma_z^B(0,y,z) + \sigma_z^C(0,y,z) \tag{4}$$

where now the σ_z^B stresses are the surface stresses measured by another method and the σ_z^C term is extracted directly from the same FEM calculation used to determine σ_x for the first contour cut. Because this method is very new, there is only a handful of examples in the literature [14,70].

5.7.2 *Cylindrical parts*

Measuring hoop stresses in a cylindrical geometry requires special attention with the contour method [71]. In a cylinder, the residual hoop stresses can have a net bending moment through the thickness of a ring. For a contour method measurement of hoop stress, a radial cut would result in excessive stresses built up at the cut tip because of the bending and moment. Such high stresses could cause plasticity errors, which have been observed for such a cut with the contour method [23] and similarly with the slitting method [72]. Different approaches have been used to deal with this issue when measuring hoop stresses in cylinders [50,71,14], including the measurements presented previously on the nuclear reactor nozzle.

5.7.3 *Miscellaneous*

A contour method measurement was performed on a specimen with only a partial-penetration weld, which resulted in a discontinuous surface contour across the unbonded interface [50,71]. A special treatment was used in the surface smoothing and FE stress calculation to handle the discontinuity. Axial stresses in cylinders and rods have been measured only rarely [34], maybe because of the difficulty in clamping such parts for a cross-sectional cut. In some work, multiaxial stress states were determined using multiple cuts and an eigenstrain analysis to reconstruct the full stress tensor [24,28].

5.7.4 *Patent*

The residual stress measurement technique described herein was invented at Los Alamos National Laboratory and is protected by United States Patent Rights (Patent Number: 6,470,756 filed February 2001, granted October 2002) until 2021. The patent is administered by the Technology Transfer Division at Los Alamos National Laboratory. Patent rights are protected in the United States only. In some circumstances, there is an “experimental use” exemption for noncommercial research. This paragraph does not constitute legal advice.

5.8 Acknowledgments

The authors would like to thank their longtime collaborator Michael R. Hill of the Univeristy of Califonia, Davis, who has been as instrumental in the development of the contour method as anyone and should have co-authored this chapter, but he was too busy writing the slitting chapter. We would like to thank Gary Schajer not only for the difficult task of editing this book but also (Prime) for years of stimulating and fruitful research interactions. We would also like to thank Lyndon Edwards, John Bouchard, Tom Holden, Phil Withers, Don Brown, Bjorn Clausen, Pierluigi Pagliaro, David Smith, C. Can Aydiner and others for valuable interactions on the contour method or residual stress in general.

Los Alamos National Laboratory is operated by the Los Alamos National Security, LLC for the National Nuclear Security Administration of the U.S. Department of Energy under contract DE-AC52-06NA25396. The U.S. Government retains a nonexclusive, royalty-free license to publish or reproduce the published form of this contribution, or to allow others to do so, for U.S. Government purposes.

5.9 References

1. Prime MB, Gonzales AR (2000) The Contour Method: Simple 2-D Mapping of Residual Stresses, The 6th International Conference on Residual Stresses, Oxford, U.K., 2000, IOM Communications, London, U.K., pp 617-624

2. Prime MB (2001) Cross-sectional mapping of residual stresses by measuring the surface contour after a cut, Journal of Engineering Materials and Technology 123 (2):162-168

3. Bueckner H (1958) The propagation of cracks and the energy of elastic deformation, Transactions of the American Society of Mechanical Engineers 80:1225-1230

4. Bueckner H (1970) Novel principle for the computation of stress intensity factors, Zeitschrift fuer Angewandte Mathematik & Mechanik 50 (9):529-546

5. Bueckner HF (1973) Field singularities and related integral representations, Sih GC (ed) Mechanics of Fracture vol 1, pp 239-314

6. Barenblatt GI (1962) The Mathematical Theory of Equilibrium Cracks in Brittle Fracture, Dryden HL, Kármán Tv, Kuerti G, Dungen FHvd, Howarth L (eds) Advances in Applied Mechanics, vol 7, Elsevier, pp 55-129. doi:10.1016/s0065-2156(08)70121-2

7. Paris PC, Gomez MP, Anderson WE (1961) A rational analytic theory of fatigue, Trends in Engineering, University of Washington 13:9-14

8. Eshelby JD (1957) The determination of the elastic field of an ellipsoidal inclusion, and related problems, Proceedings of the Royal Society of London Series A Mathematical and Physical Sciences 241 (1226):376-396

9. Tada H, Paris PC, Irwin GR (2000) The stress analysis of cracks handbook 3rd ed, The American Society of Mechanical Engineers, New York, NY

10. Prime MB, Kastengren AL (2011) The Contour Method Cutting Assumption: Error Minimization and Correction, Proulx T (ed) Experimental and Applied Mechanics, Volume 6, vol 17, Conference Proceedings of the Society for Experimental Mechanics Series, Springer New York, pp 233-250. Currently available at http://www.lanl.gov/contour/. doi:10.1007/978-1-4419-9792-0_40

11. Hosseinzadeh F, Ledgard P, Bouchard P (2013) Controlling the Cut in Contour Residual Stress Measurements of Electron Beam Welded Ti-6Al-4V Alloy Plates, Experimental Mechanics 53 (5):829-839. doi:10.1007/s11340-012-9686-1

12. Hacini L, Van Lê N, Bocher P (2009) Evaluation of Residual Stresses Induced by Robotized Hammer Peening by the Contour Method, Experimental Mechanics 49 (6):775-783

13. Frankel PG, Withers PJ, Preuss M, Wang HT, Tong J, Rugg D (2012) Residual stress fields after FOD impact on flat and aerofoil-shaped leading edges, Mechanics of Materials 55:130-145. doi:10.1016/j.mechmat.2012.08.007

14. Hosseinzadeh F, Bouchard P (2012) Mapping Multiple Components of the Residual Stress Tensor in a Large P91 Steel Pipe Girth Weld Using a Single Contour Cut, Experimental Mechanics 53 (2):171-181. doi:10.1007/s11340-012-9627-z

15. Traore Y, Bouchard P, Francis J, Hosseinzadeh F (2011) A novel cutting strategy for reducing plasticity induced errors in residual stress measurements made with the contour

method, ASME Pressure Vessels and Piping Conference, Baltimore, USA, 17-21 July, 2011, pp 1201-1212. doi:10.1115/PVP2011-57509

16. Murugan N, Narayanan R (2009) Finite element simulation of residual stresses and their measurement by contour method, Materials & Design 30 (6):2067-2071. doi:10.1016/j.matdes.2008.08.041

17. Richter-Trummer V, Moreira P, Ribeiro J, de Castro P (2011) The Contour Method for Residual Stress Determination Applied to an AA6082-T6 Friction Stir Butt Weld, Materials Science Forum 681:177-181. doi:10.4028/www.scientific.net/MSF.681.177

18. Traore Y, Paddea S, Bouchard P, Gharghouri M (2013) Measurement of the Residual Stress Tensor in a Compact Tension Weld Specimen, Experimental Mechanics 53 (4):605-618. doi:10.1007/s11340-012-9672-7

19. Hosseinzadeh F, Toparli MB, Bouchard PJ (2012) Slitting and Contour Method Residual Stress Measurements in an Edge Welded Beam, Journal of Pressure Vessel Technology 134 (1):011402-011406

20. Pagliaro P, Prime MB, Clausen B, Lovato ML, Zuccarello B (2009) Known Residual Stress Specimens Using Opposed Indentation, Journal of Engineering Materials and Technology 131:031002

21. Savaria V, Hoseini M, Bridier F, Bocher P, Arkinson P (2011) On the measurement of residual stress in induction hardened parts, Materials Science Forum 681:431-436

22. Cheng W, Finnie I, Gremaud M, Prime MB (1994) Measurement of near-surface residual-stresses using electric-discharge wire machining, Journal of Engineering Materials and Technology 116 (1):1-7

23. Johnson G (2008) Residual stress measurements using the contour method. Ph.D. Dissertation, University of Manchester. (Currently available at http://www.lanl.gov/contour),

24. DeWald AT, Hill MR (2006) Multi-axial contour method for mapping residual stresses in continuously processed bodies, Experimental Mechanics 46 (4):473-490

25. Hatamleh O, Lyons J, Forman R (2007) Laser peening and shot peening effects on fatigue life and surface roughness of friction stir welded 7075-T7351 aluminum, Fatigue and Fracture of Engineering Material and Structures 30 (2):115-130

26. Prime MB, Sebring RJ, Edwards JM, Hughes DJ, Webster PJ (2004) Laser surface-contouring and spline data-smoothing for residual stress measurement, Experimental Mechanics 44 (2):176-184

27. DeWald AT, Rankin JE, Hill MR, Lee MJ, Chen HL (2004) Assessment of Tensile Residual Stress Mitigation in Alloy 22 Welds Due to Laser Peening, Journal of Engineering Materials and Technology 126 (4):465-473

28. Kartal ME, Liljedahl CDM, Gungor S, Edwards L, Fitzpatrick ME (2008) Determination of the profile of the complete residual stress tensor in a VPPA weld using the multi-axial contour method, Acta Materialia 56 (16):4417-4428

29. Zhang Y, Ganguly S, Edwards L, Fitzpatrick ME (2004) Cross-sectional mapping of residual stresses in a VPPA weld using the contour method, Acta Materialia 52 (17):5225-5232

30. Frankel P, Preuss M, Steuwer A, Withers PJ, Bray S (2009) Comparison of residual stresses in Ti6Al4V and Ti6Al2Sn4Zr2Mo linear friction welds, Materials Science and Technology 25:640-650. doi:10.1179/174328408x332825

31. Prime MB, Hill MR (2006) Uncertainty, Model Error, and Order Selection for Series-Expanded, Residual-Stress Inverse Solutions, Journal of Engineering Materials and Technology 128 (2):175-185

32. Pagliaro P, Prime MB, Swenson H, Zuccarello B (2010) Measuring Multiple Residual-Stress Components Using the Contour Method and Multiple Cuts, Experimental Mechanics 50 (2):187-194. doi:10.1007/s11340-009-9280-3

33. Wilson GS, Grandt Jr AF, Bucci RJ, Schultz RW (2009) Exploiting bulk residual stresses to improve fatigue crack growth performance of structures, International Journal of Fatigue 31 (8-9):1286-1299

34. DeWald AT, Hill MR (2009) Eigenstrain based model for prediction of laser peening residual stresses in arbitrary 3D bodies. Part 2: model verification, Journal of Strain Analysis for Engineering Design 44 (1):13-27

35. Evans A, Johnson G, King A, Withers PJ (2007) Characterization of laser peening residual stresses in Al 7075 by synchrotron diffraction and the contour method, Journal of Neutron Research 15 (2):147-154

36. DeWald AT, Hill MR (2009) Eigenstrain based model for prediction of laser peening residual stresses in arbitrary 3D bodies. Part 1: model description, Journal of Strain Analysis for Engineering Design 44 (1):1-11

37. Pagliaro P, Prime MB, Robinson JS, Clausen B, Swenson H, Steinzig M, Zuccarello B (2011) Measuring Inaccessible Residual Stresses Using Multiple Methods and Superposition, Experimental Mechanics 51 (7):1123-1134. doi:10.1007/s11340-010-9424-5

38. Moat RJ, Pinkerton AJ, Li L, Withers PJ, Preuss M (2011) Residual stresses in laser direct metal deposited Waspaloy, Materials Science and Engineering: A 528 (6):2288-2298. doi:DOI: 10.1016/j.msea.2010.12.010

39. Rangaswamy P, Griffith ML, Prime MB, Holden TM, Rogge RB, Edwards JM, Sebring RJ (2005) Residual stresses in LENS (R) components using neutron diffraction and contour method, Materials Science and Engineering A 399 (1-2):72-83

40. Prime MB, Gnaupel-Herold T, Baumann JA, Lederich RJ, Bowden DM, Sebring RJ (2006) Residual stress measurements in a thick, dissimilar aluminum alloy friction stir weld, Acta Materialia 54 (15):4013-4021

41. Woo W, Choo H, Prime MB, Feng Z, Clausen B (2008) Microstructure, texture and residual stress in a friction-stir-processed AZ31B magnesium alloy, Acta materialia 56 (8):1701-1711

42. Zhang Y, Ganguly S, Stelmukh V, Fitzpatrick ME, Edwards L (2003) Validation of the Contour Method of Residual Stress Measurement in a MIG 2024 Weld by Neutron and Synchrotron X-ray Diffraction, Journal of Neutron Research 11 (4):181-185

43. Richter-Trummer V, Tavares SMO, Moreira P, de Figueiredo MAV, de Castro P (2008) Residual stress measurement using the contour and the sectioning methods in a MIG weld: Effects on the stress intensity factor, Ciência & Tecnologia dos Materiais 20 (1-2):114-119

44. Turski M, Edwards L (2009) Residual stress measurement of a 316L stainless steel bead-on-plate specimen utilising the contour method, International Journal of Pressure Vessels and Piping 86 (1):126-131

45. Bouchard PJ (2008) Code characterisation of weld residual stress levels and the problem of innate scatter, International Journal of Pressure Vessels and Piping 85 (3):152-165

46. Zhang Y, Pratihar S, Fitzpatrick ME, Edwards L (2005) Residual stress mapping in welds using the contour method, Materials Science Forum 490/491:294-299

47. Kartal M, Turski M, Johnson G, Fitzpatrick ME, Gungor S, Withers PJ, Edwards L (2006) Residual stress measurements in single and multi-pass groove weld specimens using neutron diffraction and the contour method, Materials Science Forum 524-525:671-676

48. Withers PJ, Turski M, Edwards L, Bouchard PJ, Buttle DJ (2008) Recent advances in residual stress measurement, The International Journal of Pressure Vessels and Piping 85 (3):118-127

49. Thibault D, Bocher P, Thomas M, Gharghouri M, Côté M (2010) Residual stress characterization in low transformation temperature 13%Cr-4%Ni stainless steel weld by neutron diffraction and the contour method, Materials Science and Engineering: A 527 (23):6205-6210. doi:DOI: 10.1016/j.msea.2010.06.035

50. Brown DW, Holden TM, Clausen B, Prime MB, Sisneros TA, Swenson H, Vaja J (2011) Critical Comparison of Two Independent Measurements of Residual Stress in an Electron-Beam Welded Uranium Cylinder: Neutron Diffraction and the Contour Method, Acta Materialia 59 (3):864-873. doi:10.1016/j.actamat.2010.09.022

51. DeWald AT, Legzdina D, Clausen B, Brown DW, Sisneros TA, Hill MR (2013) A Comparison of Residual Stress Measurements on a Linear Friction Weld Using the Contour Method and Neutron Diffraction, Ventura CE, Crone WC, Furlong C (eds) Experimental and Applied Mechanics, Volume 4, vol 34, Conference Proceedings of the Society for Experimental Mechanics Series, Springer New York, pp 183-189. doi:10.1007/978-1-4614-4226-4_22

52. DeWald AT, Hill MR, Willis E (2011) Measurement of Welding Residual Stress in Dissimilar Metal Welds Using the Contour Method, ASME Pressure Vessels and Piping Conference 2011, ASME, pp 1599-1605. doi:10.1115/PVP2011-57720

53. Kelleher J, Prime MB, Buttle D, Mummery PM, Webster PJ, Shackleton J, Withers PJ (2003) The Measurement of Residual Stress in Railway Rails by Diffraction and Other Methods, Journal of Neutron Research 11 (4):187-193

54. Schleinzer G, Fischer FD (2001) Residual stress formation during the roller straightening of railway rails, International Journal of Mechanical Sciences 43 (10):2281-2295. doi:10.1016/s0020-7403(01)00041-8

55. Ismonov S, Daniewicz SR, Newman JJC, Hill MR, Urban MR (2009) Three Dimensional Finite Element Analysis of a Split-Sleeve Cold Expansion Process, Journal of Engineering Materials and Technology 131 (3):031007. doi:10.1115/1.3120392

56. Stuart DH, Hill MR, Newman JC, Jr (2011) Correlation of one-dimensional fatigue crack growth at cold-expanded holes using linear fracture mechanics and superposition, Engineering Fracture Mechanics 78 (7):1389-1406

57. Rubio-González C, Felix-Martinez C, Gomez-Rosas G, Ocaña JL, Morales M, Porro JA (2011) Effect of laser shock processing on fatigue crack growth of duplex stainless steel, Materials Science and Engineering: A 528 (3):914-919. doi:DOI: 10.1016/j.msea.2010.10.020

58. Lillard RS, Kolman DG, Hill MA, Prime MB, Veirs DK, Worl LA, Zapp P (2009) Assessment of corrosion based failure in stainless steel containers used for the long-term storage of plutonium base salts, Corrosion 65 (3):175-186

59. Cuellar SD, Hill MR, DeWald AT, Rankin JE (2012) Residual stress and fatigue life in laser shock peened open hole samples, International Journal of Fatigue 44:8-13. doi:10.1016/j.ijfatigue.2012.06.011

60. Richter-Trummer V, Suzano E, Beltrao M, Roos A, dos Santos JF, de Castro PMST (2012) Influence of the FSW clamping force on the final distortion and residual stress field, Materials Science and Engineering A 538:81-88. doi:10.1016/j.msea.2012.01.016

61. Carlone P, Palazzo GS (2012) Experimental Analysis of the Influence of Process Parameters on Residual Stress in AA2024-T3 Friction Stir Welds, Key Engineering Materials 504-506:753-758. doi:10.4028/www.scientific.net/KEM.504-506.753

62. Boyce BL, Reu PL, Robino CV (2006) The constitutive behavior of laser welds in 304L stainless steel determined by digital image correlation, Metallurgical and Materials Transactions A 37A (8):2481-2492

63. Shin SH (2005) FEM analysis of plasticity-induced error on measurement of welding residual stress by the contour method, Journal of Mechanical Science and Technology 19 (10):1885-1890

64. Dennis RJ, Bray DP, Leggatt NA, Turski M (2011) Assessment of the influence of plasticity and constraint on measured residual stresses using the contour method, ASME Pressure Vessels and Piping Division Conference, Chicago, IL, USA, 2008, ASME, pp 477-485. doi:10.1115/PVP2008-61490

65. Edwards L, Smith M, Turski M, Fitzpatrick M, Bouchard P (2008) Advances in residual stress modeling and measurement for the structural integrity assessment of welded thermal power plant, Advanced Materials Research 41-42:391-400

66. Prime MB (2010) Plasticity effects in incremental slitting measurement of residual stresses, Engineering Fracture Mechanics 77 (10):1552-1566. doi:10.1016/j.engfracmech.2010.04.031

67. Pagliaro P, Prime MB, Zuccarello B (2007) Inverting multiple residual stress components from multiple cuts with the contour method, SEM Annual Conference and Exposition on Experimental and Applied Mechanics, 2007, pp 1993-2005

68. Wong W, Hill MR (2012) Superposition and Destructive Residual Stress Measurements, Experimental Mechanics 53 (3):339-344. doi:10.1007/s11340-012-9636-y

69. Prime MB, Newborn MA, Balog JA (2003) Quenching and cold-work residual stresses in aluminum hand forgings: contour method measurement and FEM prediction, Materials Science Forum 426-432:435-440

70. Olson MD, Wong W, Hill MR (2012) Simulation of Triaxial Residual Stress Mapping for a Hollow Cylinder, ASME 2012 Pressure Vessels & Piping Division Conference, Toronto, Ontario, CANADA, 2012, pp PVP-2012-78885

71. Prime MB (2011) Contour Method Advanced Applications: Hoop Stresses in Cylinders and Discontinuities. Paper presented at the Engineering Applications of Residual Stress, Volume 8, doi:10.1007/978-1-4614-0225-1_2

72. de Swardt RR (2003) Finite element simulation of crack compliance experiments to measure residual stresses in thick-walled cylinders, Journal of Pressure Vessel Technology 125 (3):305-308